Insertion loss due to a magnetically permeable spherical shell covering a concentric conducting target

P. D. Saraf and D. Indira Nagubai
National Geophysical Research Institute, Hyderabad, India.

Received: 15 October, 1991; accepted: 6 October, 1992.

RESUMEN

Se considera un modelo estratificado de dos esferas concéntricas en contacto no galvánico, que representan un cuerpo mineral conductor rodeado de un halo de roca alterada. Se demuestra que: (a) un cambio en las propiedades de la roca madre o de las formaciones mineralizadas distorsiona los parámetros electromagnéticos y puede modificar la sensibilidad de detección en ciertas bandas de frecuencias; (b) las mediciones a varias frecuencias permiten penetrar debajo de una capa de alta conductividad; (c) el parámetro de blindaje presenta patrones diferentes de variaciones de frecuencia según la conductividad de la cubierta, lo que ayuda a distinguir las anomalías electromagnéticas para cada tipo de cubierta. Estos resultados pueden servir para: 1. comprender el fenómeno de blindaje en situaciones geológicas complejas; 2. generar información de base para la planeación de experimentos electromagnéticos en la exploración minera.

PALABRAS CLAVE: Método electromagnético, exploración minera.

ABSTRACT

A layered section in a uniform electromagnetic field is assumed to have two concentric spherical shells (in nongalvanic contact). Such targets may occur in native copper deposits viz., conducting ore bodies surrounded by a halo of altered rocks. It is found that (a) changes in characteristic properties of overburden and/or ore formations cause significant distortions in the geoelectromagnetic parameters and may change the detection sensitivity in some bands of frequencies; (b) multifrequency measurements afford the possibility of seeing beneath highly conducting layers; and (c) the variation of the shielding parameter with frequency exhibits, qualitatively, different patterns for conductive and resistive covers and may help distinguishing EM anomalies due to conductive and resistive overburden formations. The results may be useful in (1) understanding the shielding phenomenon in complex geological situations, and (2) providing background information (i.e. shielding behaviour of overlying or surrounding formations) against which geoelectromagnetic experiments can be planned.

KEY WORDS: Electro-magnetic survey, mineral exploration.

INTRODUCTION

In geoelectromagnetic field measurements the target bodies are usually concealed by overburden. The shielding effectiveness of the overburden must be taken into account. This includes (i) choosing the frequency ranges serving as discrimination windows for favourable and unfavourable conditions of transmission of signals from the target and surroundings, and (ii) accounting for the changes in the physical/geometrical parameters of cover-target system such that the inducing or secondary fields may penetrate overlying formations. The shielding effects of overlying formations have close relevance to ore identification and evaluation of the effect of surrounding formations. Much work has been done on EM shielding effectiveness in radio frequency ranges, using both theoretical and experimental approaches. Bannister (1968) used this concept for geophysical investigations in quasi-near field ranges. Negi *et al.*, (1976) and Negi and Saraf (1986) extended the studies to shell-sphere and plane layered models, respectively.

In this paper, an attempt is made to study the shielding effectiveness of overburden formations in multifrequency EM measurements. The model consists of two concentric thin shells (in nongalvanic contact) representing alteration and mineralization zoning (viz., porphyry copper deposits having disseminated mineralisation, emplaced in host rocks and altered hydrothermal solutions; Lowell (1968)). Quantitative estimates of shielding due to changes in physical and geometrical properties of overburden-ore formations in various frequency ranges are given.

FORMULATION

The physical system is shown in Figure 1. It consists of two concentric spherical shells of radii 'B' (outer) and 'A' (inner); thicknesses D_1 (outer) and D_2 (inner); conductivities σ_1 (outer) and σ_2 (inner); magnetic permeabilities μ_1 (outer) and μ_2 (inner) and dielectric permittivities ε_1 (outer) and ε_2 (inner). The system is assumed to be excited by uniform EM fields.

Following Negi and Saraf (1984) the reflection factor for the composite two shell spherical system is given by:

$$R\Big|_{\text{composite}} = \left[1 - \left\{\frac{3(1+P_{II})}{3 + r_{II}BD_1(1+P_{II})}\right\}\right] \quad (1)$$

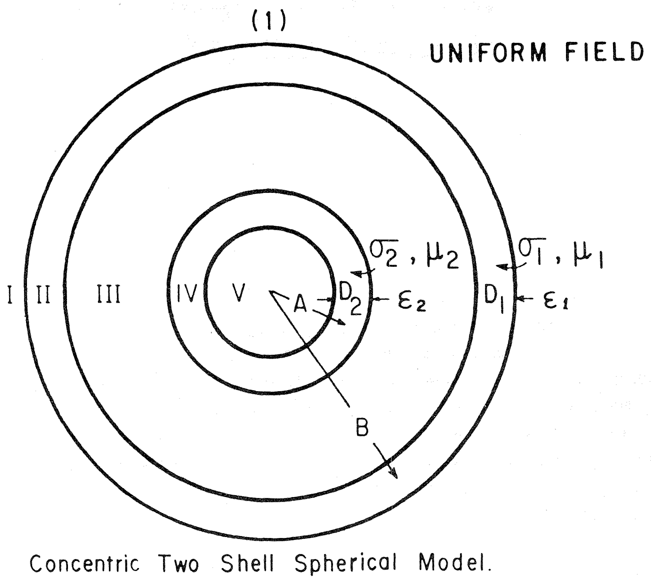

Fig. 1. Concentric shells in uniform EM fields.

where

$$P_H = \frac{r_{IV} \cdot A \cdot D_2}{3 + r_{IV} A D_2} \left(\frac{A}{B}\right)^3 ;$$

$r_{II} = i\,\omega\,\mu_1\,(\sigma_1 + i\,\omega\,\varepsilon_1)$; $r_{IV} = i\,\omega\,\mu_2\,(\sigma_2 + i\,\omega\,\varepsilon_2)$;

$\omega = 2\,\pi\,F$ and, F = frequency of the incident EM waves.

From equation (1) the expression for the reflection factor $R|_{target}$ can be written as:

$$R|_{target} = \frac{r_{IV}\ A \cdot D_2}{3 + r_{IV} AD_2} \qquad (2)$$

Following Negi and Saraf (1986) the shielding effectiveness (δ) parameter can be defined as

$$\delta = 20 \text{ Log}_{10} \frac{|R|\ \text{target}}{|R|\ \text{composite}} \text{ in db} \qquad (3)$$

Values of $|R|_{target}$ and $|R|_{composite}$ have been obtained from equations (2) and (1), respectively.

This insertion loss approach has been utilised extensively (using equation 3) in EM compatibility literature. It is also realised that variation of shielding effectiveness parameter with frequency of EM waves provide an effective and sensitive tool to demonstrate the optimum shield for a given set of physical and geometrical constraints of the model. It has the potential to provide a priori information in planning EM experiments in complex geological situations.

DISCUSSION

Some representative numerical results have been obtained to show the variation of shielding effectiveness (δ) with frequency of the EM waves for changes in the values of geometrical (B/A, D_1, D_2) and physical (σ_1, σ_2; μ_1, μ_2, ε_1) parameters of the system.

(I) Change of radius of cover (B)

Here the radius of the target is kept constant (A = 100 m) and the radius of the cover (B = 100 m, 150 m, 200 m) has been changed. The shielding effectiveness parameter (δ) has been plotted assuming that the inner shell is 10^3 times more conducting than the outer shell. Such situations may occur where native sulphide deposits are surrounded by a halo of less conducting material. This may be due to irregular density, higher porosity, different fluid permeability, salt concentration etc. The salient features of Figure 2(a) are discussed as below:

(a) Curve No. 1: In this case A = B = 100 m and the system behaves like a single shell model. A value of $\delta = -10$ indicates the situation where a conducting shell of thickness D_1 surrounds a halo of resistive space of radius A. The negative sign in the 'δ' value is caused by the waves reflecting from the interfaces of the shell (Schulz *et al.*, 1968).

(b) Curves Nos. 2 and 3: Conductivity contrast between the target and cover is now of the order of 10^3 (Figure 2a). The outer cover with conductivity value 10^{-3} allows a major portion of EM energy to penetrate the cover in the frequency range $F<10^4$ Hz. In this frequency range the characteristics of the cover (B = 150 M, A = 100 M) will be dominated by the presence of a highly conducting target and thus affect the shielding effectiveness of the cover. When the cover is taken away, the effect of the target on the shielding behaviour of the cover decreases. This results in an increase in the shielding parameter. A conducting layer at a distance of B = 200 meters from the highly conducting target has a better shielding property in low-frequency range ($F<10^4$ Hz) than the corresponding situation of B = 150 m. Hence in the interpretation of geoelectromagnetic data the shielding due to surrounding formations must be given due considerations more particularly in delineating highly conducting targets by multifrequency electromagnetic measurements. In the low-frequency range ($F<10^4$Hz) the contrast in the conductivities of cover and target plays a dominant role in the shielding behaviour of the overburden formations in comparison to the geometrical distance between them.

However, when $F>10^4$ Hz, the outer shell may act as a better shield resulting into a lessened penetration of EM energy. Under such circumstances conditions of normal shielding obtain.

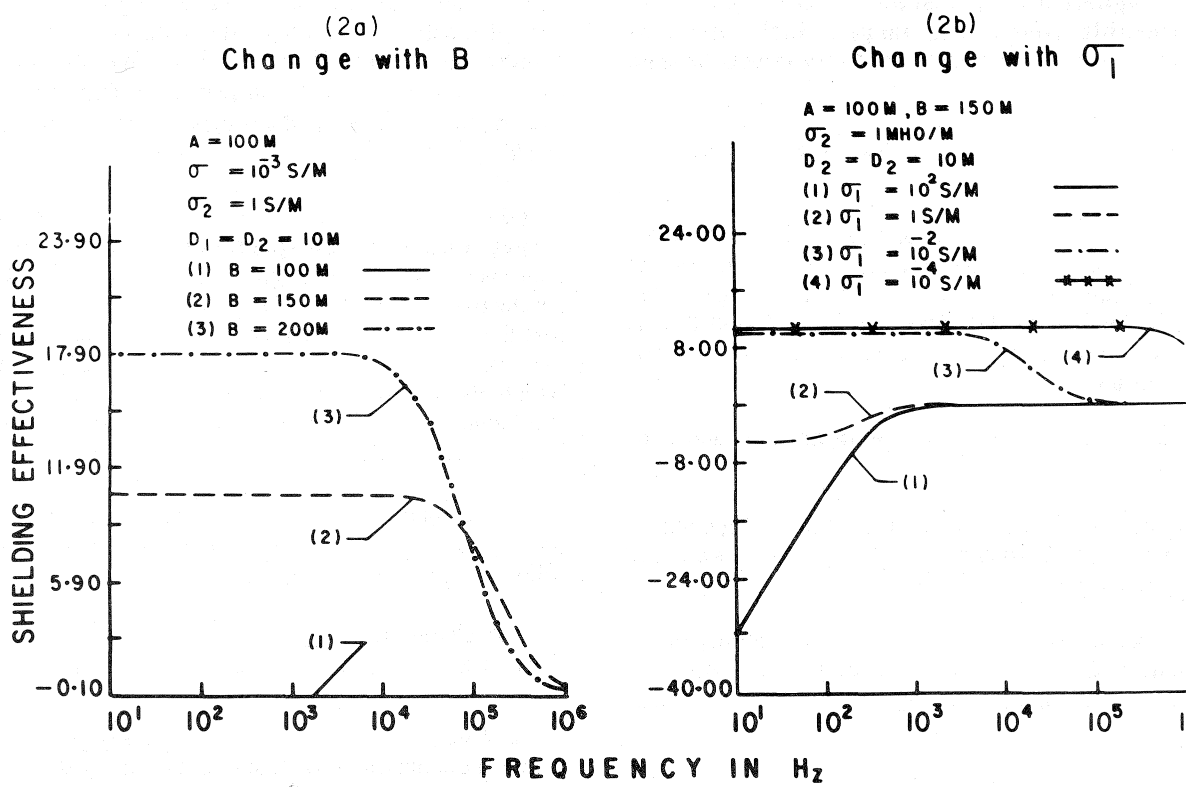

Fig. 2 (a). Variation of shielding effectiveness with frequency for different thickness of the outer shell (B = 100 m, 150 m and 200 m). (b). Variation of shielding effectiveness with frequency for different values of the conductivity in the outer shell ($\sigma_1 = 10^2$, 1, 10^{-2}, 10^{-4} MHOS/m).

(II) Change of σ_1 (keeping σ_2 constant)

Shielding behaviour for different conducting values of the overburden formations in different frequency ranges is shown in Figure 2(b). Conductivity of the target σ_2 is assumed to be constant and equal to 1 S/m. Each curve in Figure 2(b) represents different conductivity contrasts between cover and target and hence needs to be discussed individually.

(a) Curve No. 1: Here the overlying formations with higher conductivity cover a target of less conducting material. According to Parasnis (1973) "Certain overburdens (clays) may be as good conductors as some ore bodies, and conversely, ores (galena) may be as poor conductors as overburden like moraine". In such situations the conductivity of the overburden may be larger than the ore body's. It is difficult to distinghish between overburden and ore effects in such cases, e.g. when searching for sulphide deposits under highly conducting marine formations. Multifrequency measurements afford the possibility of seeing beneath highly conducting layers as in curve (1), Figure 2(b).

(b) Curve No. 2: Usually geoelectromagnetic measurements fail to identify low-contrast conductors. However, curve No. 2, Figure 2(b) shows a slight decrease in the low-frequency band ($F<10^2$ Hz) and thus illustrates the shielding behaviour of overlying conductors in non-galvanic contact. Effects of shielding should not be ignored even where the cover-target system lacks conductivity contrast.

(c) Curves Nos. 3 and 4: ($\sigma_1 = 10^{-2}$ and 10^{-4} S/m). These situations were discussed in Figure 2(a) where a less conducting outer shell covers a conducting target. Here one finds a positive value of δ. Comparison of the curves (1) and (3) reveals that for conductive (negative δ) and resistive (positive δ) covers the shielding exhibits qualitatively different patterns. This observation may be helpful in distinguishing EM anomalies due to poorly conducting overburden covering a conducting target (curve No. 3), from anomalies due to a conducting overburden covering poorly conducting ores (curve No. 1).

(III) Change with magnetic permeability

Understanding the effects of magnetic permeability is essential when searching for magnetic ores, sulphide ores, and other geological bodies containing magnetite or pyrrohotite (blackshales, basic and ultrabasic rocks). In this section changes in the magnetic behaviour of the cover or the target are discussed for different frequency ranges and combinations of cover-target systems.

(A) Magnetically permeable cover (μ_1) over non-permeable conducting target. Such situations usually occur for conducting sedimentary targets beneath basaltic formations.

i) Contrast in magnetic permeabilities only, i.e. $\mu_1 \geq \mu_a$; $\sigma_1 = \sigma_2$, $\mu_2 = 0$.

In Figure 3(a), both cover and target have the same conductivity values, i.e. the change in the value of the shielding parameter, is mainly due to the change in the magnetic behaviour of the outer shell. It is found that as the magnetic value of the cover increases the shielding parameter does too.

ii) Contrast in both magnetic permeabilities and conductivities.

In Figure 3(b) the combined effect of changing conductivity and magnetic permeability contrasts are shown in the frequency range 10^1 Hz to 10^6 Hz.

The effect of changing μ_1 (magnetic permeability of the outer shell) occurs in the frequency range $F>10^4$ Hz only. This is because changes in the properties of the cover can be seen only in the high frequency range.

As μ_1 increases, unlike Figure 3(a), the shielding parameter decreases. The model in Figure 3(b) represents a case of Pure Magnetic Shielding. A magnetic shield has a sort of electric core, where the induced currents try to counter-balance the effects due to the magnetic properties of the cover. If the core is highly conducting (i.e. $\sigma_2 = 1$ s/m, $\sigma_1 = 10^{-3}$ s/m), it decreases the effect of magnetic shield.

(B) Magnetically permeable conducting target under a non-permeable cover. Here the combined effects of changing magnetic permeability and conductivity of the target body is discussed. It is assumed that the cover is non-permeable and less conducting than the target. This resembles the case of an electric shield in which the magnetic core is covered by an electrically conducting layer. The efficiency of shielding increases for higher values of μ_2.

On comparing the numerical results of Figure 3(b), (change of μ_1) and Figure 4 (change of μ_2) one finds the following qualitative changes.

i) A change in μ_1 is seen only in the frequency range $F>10^4$ Hz, while a change in μ_2 is observed in $F< 10^4$Hz.

ii) When the outer shell is magnetically permeable and covers a conducting target, an increase in μ_1 decreases the shielding parameter, while an increase in μ_2 increases the shielding effectiveness.

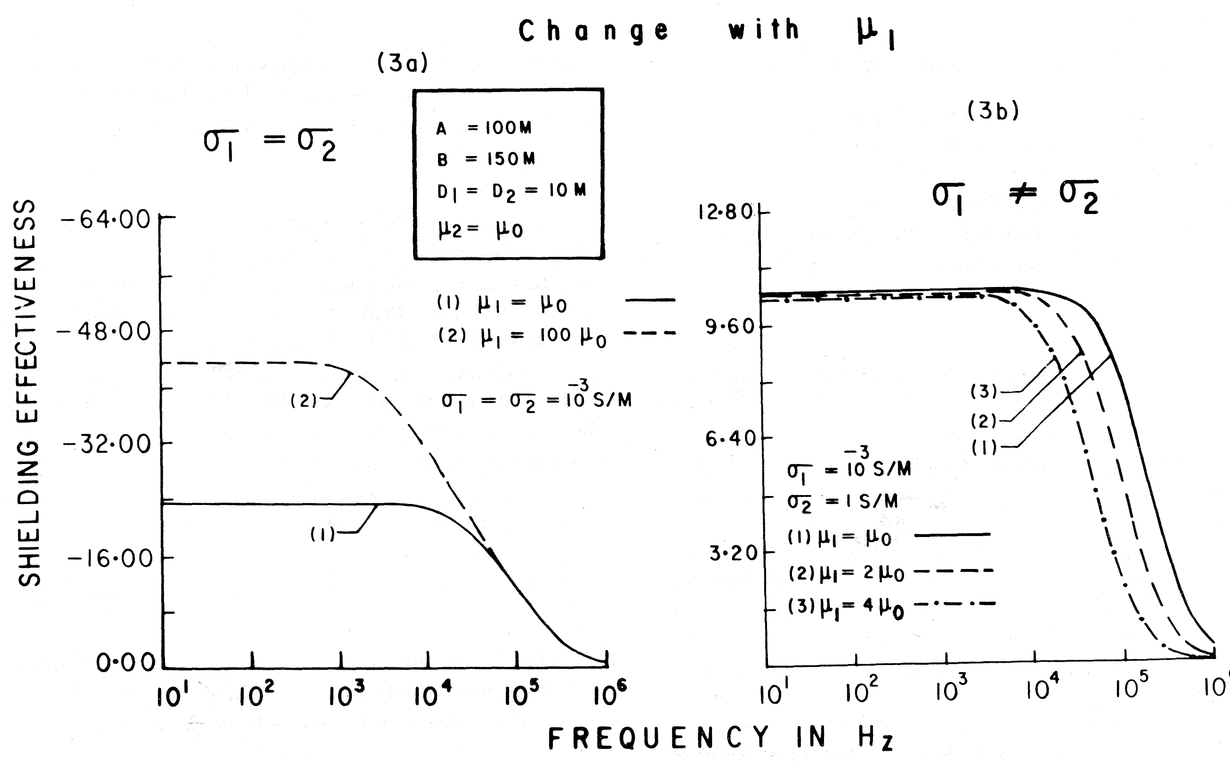

Fig. 3(a). Variation of shielding effectiveness with frequency for different values of the magnetic permeability in the outer shell (i.e. $\mu_1 = \mu_o$, 100 μ_o) for $\sigma_1 = \sigma_2$. (b). Variation of shielding effectiveness with frequency for different values of the magnetic permeability in the outer shell ($\mu_1 = \mu_o$, 2 μ_o and 4 μ_o) and $\sigma_1 \neq \sigma_2$.

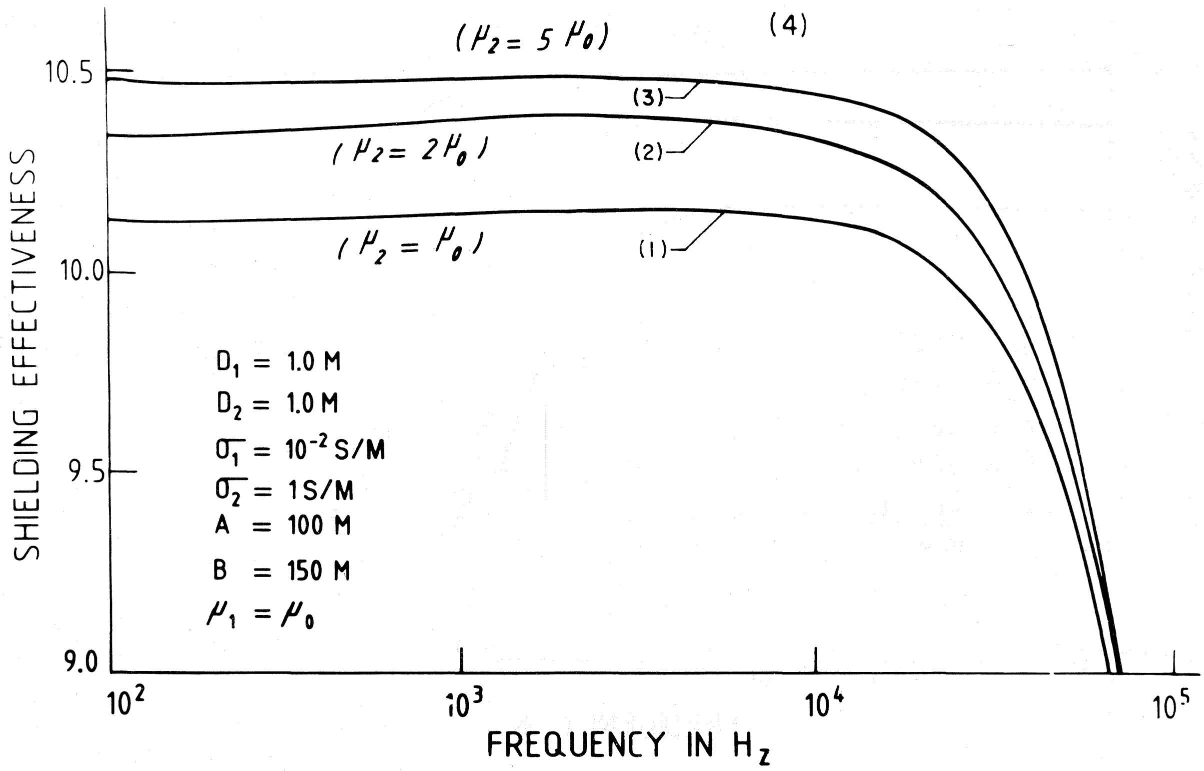

Fig. 4. Variation of shielding effectiveness with frequency for different values of the magnetic permeability in the inner shell ($\mu 2 = \mu_o$, 2 μ_o and 5 μ_o) and $\sigma 1 \neq \sigma 2$.

(IV) Change of dielectric permittivity (ε_1):

Now both shells are equally resistive ($\sigma_1 = \sigma_2 = 10^{-4}$ S/M). The dielectric permittivities of the target and cover are assumed to be ε_o and ε_1 (50 ε_o, 100 ε_o). Such conditions may occur in glaciated conditions of Scandinavia or Canada.

One finds a sharp kink in the δ–F variation pattern. The kink shifts towards lower frequency bands with an increase in the ε_1 value. Such kinks are not observed when only the electrical conductivity or magnetic permeability values of the cover change. They may serve as a diagnostic tool for mapping targets beneath a medium with high dielectric permittivity.

(V) Change in thickness of the shells D_1 or D_2

The thickness of the overlying disseminated zone may be large enough to mask the response of a massive ore deposits.

In Figure 6, the shielding behaviour of the outer shell with varying thicknesses is described. As in Figure 2(b), we find that the conductivity contrast between cover and target plays a dominant role in comparison to the change in the thickness of the overlying formations. Shielding due to an outer shell with thickness D_1 = 10m will be less than the corresponding situation with D_1 = 2m. In both cases the target was assumed to be 10^2 times more conducting than the overburden.

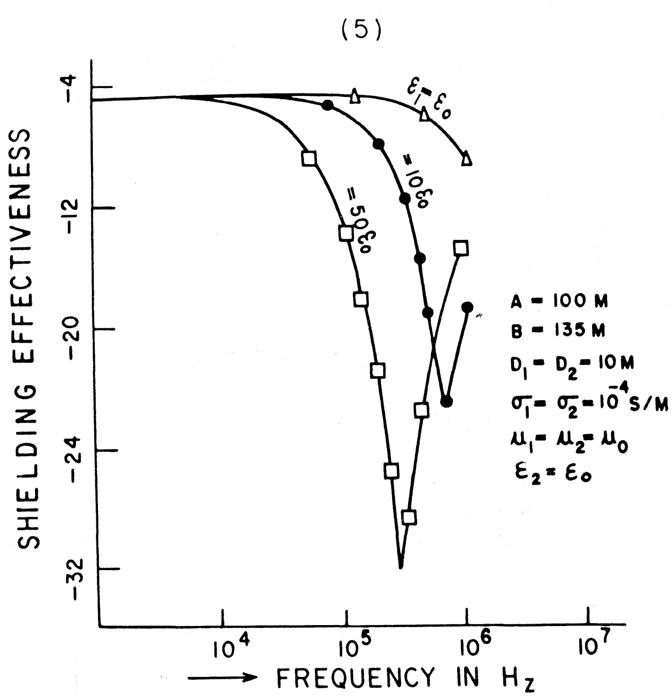

Fig. 5. Variation of shielding effectiveness with frequency for different values of the dielectric permittivity in the outer shell ($\varepsilon 1 = \varepsilon_o$, 10 ε_o, 50 ε_o).

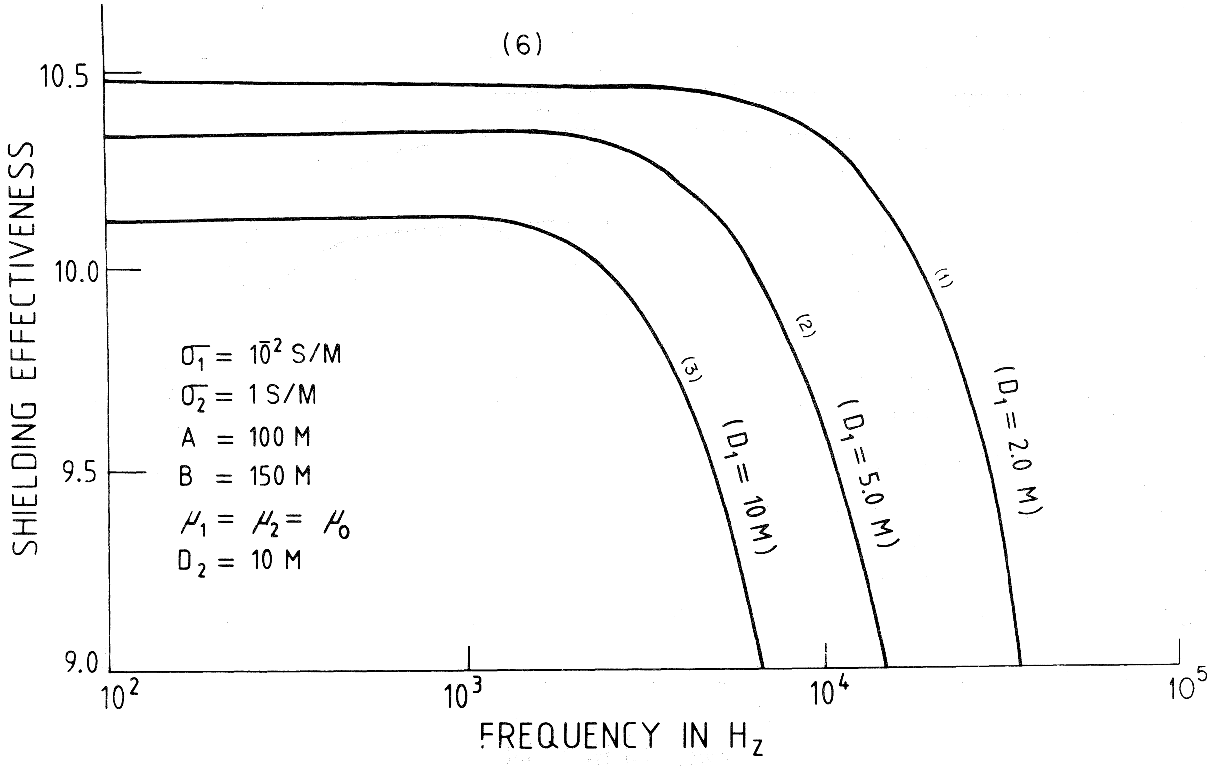

Fig. 6. Variation of shielding effectiveness against frequency for different thickness of the outer shell (D1 = 2m, 5m, 10m).

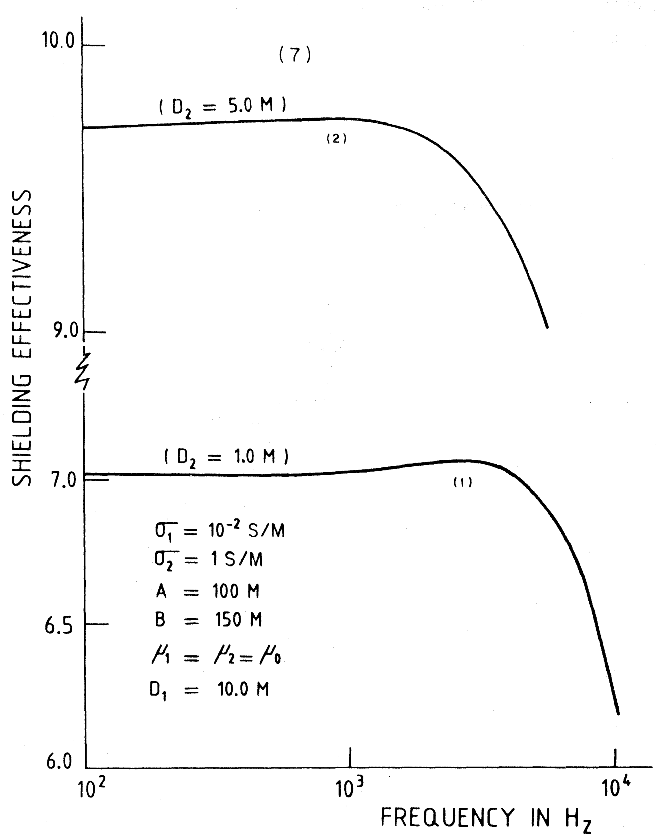

Fig. 7. Variation of shielding effectiveness against frequency for different thickness of the inner shell (D2 = 1m and 5m).

In Figure 7, the thickness of the outer shell is kept constant at D_1 = 10m, and the thickness of the inner shell varies. Here again the conductivity and the thickness of the inner shell plays a dominant role. The thicker the target the higher is the shielding parameter.

CONCLUSIONS

We have discussed various combinations of cover-target systems in uniform EM fields. The results show the shielding effectiveness of the overlying formation in different frequency ranges. Sensitivity of the shielding parameter to changes in the physical and/or geometrical parameters have been highlighted. We show that in interpretation of EM induction prospecting data one ought to give equal importance to the changes in the physical and geometrical properties of both the conducting target and the overlying formations.

ACKNOWLEDGEMENTS

The authors are grateful to Dr. R. N. Singh for his encouragement and discussions. The help extended by Mr. D. V. Subrahmanyam in the preparation of the manuscript is thankfully acknowledged. The authors wish to thank the Director, National Geophysical Research Institute, Hyderabad for his kind permission to publish this work.

BIBLIOGRAPHY

PARASNIS, D. S., 1973. Mining Geophysics. (Elsevier, Amsterdam.

SCHULZ, R. B., V. C. PLANTZ and D. R. BRUSH, 1968. Low frequency shielding resonance. *IEEE Trans, on EM compatibility, EMC10, 1*, 7-15.

NAGUBAI, D. I. and P. D. SARAF, 1993. Multifrequency electromagnetic response of a permeable cover target system. Bolletino di Geofisica. (In press).

NAGUBAI, D. I. and P. D. SARAF, 1991. Response resolution of shielded conductors through multifrequency EM measurements. A review Indo-US Workshop on EM Induction, Jan 13-14, 1991 held at IIT, Kharagpur, West Bengal.

NEGI, J. G., K. N. RAO and U. RAVAL, 1976. Insertion loss due to spherical shell in low-frequency zone. *IEEE Trans., on Ant. and Wave Propagation, Vol. AP 12(4)*, 389-392.

NEGI, J. G. and P.D. SARAF, 1984. Multifrequency electromagnetic response of a shielded conductor, *Geophys. Int., 23*, 1, 1-15.

P. D. Saraf and D. Indira Nagubai
National Geophysical Research Institute
Hyderabad-500 007 (A. P.)
INDIA